Mechanism of Nitrite Transporter NirC in Motility, Biofilm Formation, and Adhesion of Avian Pathogenic Escherichia Coli

Jiaqi Liu
Yangzhou University
Dong Zhang
Yangzhou University
Siqi Lian
Yangzhou University
Xuanqiang Gu
Yangzhou University
Qianxi Hou
Yangzhou University
Pengpeng Xia
Yangzhou University
Guoqiang Zhu (yzgqzhu@yzu.edu.cn)
Yangzhou University https://orcid.org/0000-0002-5491-0670

Research Article

Keywords: avian pathogenic Escherichia coli (APEC), nirC, nitrite stress, 3',5'-cyclic diguanosine monophosphate (c-di-GMP)

Posted Date: April 3rd, 2021

DOI: https://doi.org/10.21203/rs.3.rs-371196/v1

Abstract

The *Escherichia coli* (*E. coli*) *nirC* gene encodes a nitrite transporter, which involved in transporting toxic nitrite (NO_2^-) from the environment into the bacteria. Although the deletion of *nirC* gene could cause changes in motility, adhesion in the previous study, and the virulence involved in the specified mechanism for pathogenic *E. coli* remains to be known. In the present work, we aimed to evaluate the role of NirC in a serotype O2:K1:H7 avian pathogenic *Escherichia coli* (APEC) strain. For this purpose, we generated a NirC-deficient mutant of APEC XM strain and examined its biological characteristics. The *nirC* gene deletion mutant enhanced ability of motility, decreased in biofilm formation, and it markedly reduced ability to adhere mouse brain microvascular endothelial cell b.End3 cells. For understanding its mechanism, sequentially we detected and found the stress regulator *rpoS* and its downstream genes *csrA* were up-regulated in NirC-deficient mutant while diguanylate cyclase gene *dgcT* was down-regulated. By high-performance liquid chromatography (HPLC) experiment, we demonstrated the concentration of intracellular 3',5'-cyclic diguanosine monophosphate (c-di-GMP) significantly decrease in *nirC* gene deletion mutant. Taken data together, we may make a conclusion with a possible signal pathway clue, due to NirC mutation, environmental NO_2^- accumulation leads to nitrite stress and inactivates c-di-GMP synthesis by stimulating the stress regulator RpoS, resulting in changes of biological characteristics.

1 Introduction

Avian pathogenic *Escherichia coli* (APEC) has a lot of serotypes, which can cause avian colibacillosis (Dho-Moulin and Fairbrother 1999). Some serotypes of APEC are highly homologous with the neonatal meningitis *Escherichia coli* (NMEC) and were applied to construct meningitis disease models in mammals. Therefore, these APEC are potential zoonotic pathogens, such as the APEC strain XM used in this study (Ma et al. 2014).

Nitrite (NO_2^-) accumulates in large amounts can produce extremely toxic molecules, such as nitric oxide (NO) and peroxynitrite anion ($ONOO^-$) (Carlsson et al. 2001). However, *E. coli* can reduce them to non-toxic ammonium through periplasmic or cytoplasmic NO_2^- reductase systems and provide electron acceptors for electron transport chain (Khlebodarova et al. 2016; Wang and Gunsalus 2000). Three kinds of NO_2^- transporters involved in NO_2^- transmembrane passage had been discovered in *E. coli*, including NirC, NarK, and NarU, and study have shown that NirC has the highest transport efficiency (Jia et al. 2009). NirC is a pentamer transmembrane protein that belongs to the formate-nitrite transporter family (Lu et al. 2012). Previously, researchers had different views on the function of NirC. Clegg and his coleagues showed NirC has the function of transferring NO_2^- into or out of bacteria (Clegg et al. 2002), while another study believed that NirC is a NO_2^-/H^+ antiporter (Rycovska et al. 2012). Later, Lu et al. (2012) utilized the structural analysis and electrophysiological detection of NirC protein, and showed that NirC is a monovalent anion channel, which has a preference for the intracellular transport of NO_2^-.

The 3',5'-cyclic diguanosine monophosphate (c-di-GMP) is one of the second messengers found in bacteria, cyclized by diguanylate cyclases with two molecules of guanosine triphosphate and degraded by specific c-di-GMP phosphodiesterase (Hengge 2009). The c-di-GMP level in cytoplasm affects changes of biological characteristics due to specific protein domain can bind c-di-GMP and control its functionality. For example, c-di-GMP can activate flagellar molecular brake protein YcgR to shut down motility of flagellar and inhibit bacterial swimming, and it can also bind cellulose synthase to increase the production of cellulose, a main component of biofilm (Cheang et al. 2019). Generally speaking, the increase of intracellular c-di-GMP concentration leads to decreased motility and enhanced biofilm formation (Simm et al. 2004).

In recent years, some progress has been reported that NirC was involved in the pathogenicity of *E. coli* (Das et al. 2009; de Paiva et al. 2015). For example, the absence of *nirC* gene can transform a strain of APEC causing swollen head syndrome into chronic infection in chicks and decrease the adhesion ability to chicken embryo fibroblasts(de Paiva et al. 2015). However, the regulatory mechanism is not clear. For understanding the mechanism of NirC on the biological characteristics of APEC, a *nirC* mutant strain was generated from the APEC strain XM in this study. By detecting the biological characteristics of the mutant, the role of NirC in APEC biological characteristics was determined. The main purpose of this study is to provide a possible explanation for NirC contributed to the motility, biofilm formation, and adhesion of pathogenic *E. coli*.

2 Materials And Methods

2.1 Bacterial strains, plasmids, cell and culture conditions

APEC XM strain was presented by Professor Lu Chengping (Nanjing Agricultural University, College of Veterinary Medicine, China) (Ma et al. 2014), and cloning *E. coli* strain DH-5α was stocked in our laboratory. APEC XM Δ*nirC* is a nirC in-frame gene mutant of APEC XM and complementary strain APEC XM Δ*nirC*/p*nirC* is an APEC XM Δ*nirC* carrying pBR322-*nirC* plasmid. All bacterial strains were grown in Luria-Bertani (LB) broth at 30 ℃ or 37 ℃ according to the request of the experiments. Plasmids pKD3, pKD46, pCP20 used for the λ Red-based recombination are stocked in our laboratory. pBR322 plasmids are used as the expression vector and purchased from Takara (Shiga, Japan).

Mouse brain microvascular endothelial cell bEnd.3 was also presented by Professor Lu Chengping(Hejair et al. 2017), and cultured in Dulbecco's modified Eagle's medium (DMEM) with low sugar (HyClone, Logan, USA), supplemented with 12% fetal bovine serum (FBS) (Gibco BRL, AUS). Cells were maintained at 37 ℃ in the incubator with 5% CO_2.

2.2 Construction of *nirC* gene mutant and complemented strain of APEC XM

APEC XM Δ*nirC* was constructed via λ Red-based recombination system (Datsenko and Wanner 2000) and the primers used are shown in Table 1. P1/P2 and P3/P4 were used to construct APEC XM Δ*nirC* with

pKD3, pKD46, and pCP20, P5/P6 was used to construct the vector pBR322-*nirC*. The Δ*nirC* and complemented strain Δ*nirC*/p*nirC* of APEC XM were confirmed by polymerase chain reaction (PCR) and DNA sequencing.

Table 1
The sequence of primers for constructing mutant and complemented strain for *nirC*

primer	sequence (5'→3')	length of PCR product/bp
P1	GTCTTGGGATCATCCTGATTTT	662
P2	CTTTCGGCGTAGCATACCA	
P3	TAATTTGCTCGACCCGTCCGTACGTCCTCTGGTGATG GGCGCGACCTTTGTGTGTAGGCTGGAGCTGCT TCG	1113
P4	CTGATAAAGTATTACCCAGCGTCACCCACAGCAGGT TATGACCAATACCCCATATGAATATCCTCCTTAG	
P5	CGCGGATCCATGTTTACAGACACTATTACTAAGTGTG	816
P6	ACGCGTCGACTTAACCGGCAGCCGTTTC	

2.3 Bacterial growth test

To understanding the growth rate of APEC XM wild type (WT), APEC XM Δ*nirC*, and APEC XM Δ*nirC*/p*nirC*, bacterial strains were cultured at 30 ℃ and 37 ℃ in 50 mL LB broth with shaking speed of 200 rpm, respectively. The cell density was estimated by measuring the optical density at 600 nm (OD_{600}) every 1 h until the value of OD_{600} was stabilized.

2.4 Motility test

The semisolid medium was prepared according to the literature method (Pesavento et al. 2008). The bacterial strains were transferred to fresh LB broth and cultured at 30℃ and 37 ℃ for 200 rpm to OD_{600} = 1.0, respectively. 0.2 μL bacterium solution (1×10^8 CFU) was added to semisolid medium and cultured at 30℃ and 37 ℃ for 24 h, the diameter of swimming zone was measured.

2.5 Crystal violet method for quantification of biofilm formation

The biofilm induction solution was prepared(Hossain and Tsuyumu 2006), bacterial strains were cultured at 30℃ and 37 ℃ without shaking for 24 h, respectively, then gently wash off the bacterial solution twice with distilled water and dye 20 min with 1% crystal violet solution. Add 95% ethanol solution to dissolve the crystal violet, and detect the absorbance at 600 nm.

2.6 Bacterial adhesion assay

The methyl thiazolyl tetrazolium (MTT) method was used in the bacterial adhesion assay with a little alteration (de Paiva et al. 2015). The bEnd.3 cells were digested and transferred to a 96-well plate at 100 µL per well. After cells covered the bottom, bacterial solution of WT, Δ*nirC*, and Δ*nirC*/p*nirC* with PBS washing twice was added to the well, respectively, according to the proportion of multiplicity of infection (MOI) = 100:1. Bacteria and cells were co-incubated at 37 ℃ for 1 h and set up a control group without bacterial treatment. Washing off each well twice by PBS and 50 µL of 5 mg/mL MTT (Solarbio, Beijing, China) dissolved by PBS was added to each well and incubated at 37 ℃ in the incubator for 12 h, so that MTT was fully reduced to Formazan by bacteria. The supernatant was gently absorbed the next day, and 50 µL of 2 mg/mL lysozyme dissolved by PBS was added to each well and incubated at 37 ℃ for 10 minutes. Then adding 250 µL dimethyl sulfoxide (DMSO) to each well and detect the absorbance of 490 nm.

2.7 Assays of the red, dry, and rough (rdar) colony morphology using Congo red plate

Bacteria can show different colony phenotypes through the differential expression of Curli and cellulose when growing in Congo red agar plate without salt, and in order to increase the contrast, Coomassie brilliant blue needs to be added. Configuration of congo red (Solarbio, Beijing, China)-coomassie brilliant blue (Solarbio, Beijing, China) salt-free medium (containing 1 g peptone, 0.5 g yeast extract, 4 mg congo red, and 2 mg coomassie brilliant blue G-250, per 100 mL water) (Jain and Chen 2006). After the bacterial strains grew to OD_{600} = 1, 2.5 µL bacteria solution was added to congo red-coomassie brilliant blue salt-free medium, and the colony morphology was observed after being cultured at 30 ℃ and 37 ℃ for 3 days.

2.8 High-performance liquid chromatography (HPLC)-based detection and quantitation of cellular c-di-GMP

2.8.1 Cellular c-di-GMP extraction

The bacterial strains were cultured at 30 ℃ and 37 ℃, and obtain a bacterial culture volume equivalent to 1 mL of OD_{600} = 2.5. The bacteria solution was centrifuged at 4 ℃ and 16000 g for 2 min, and the supernatant was discarded, and then wash the cell pellet with 1 mL ice-cold PBS twice. After discarding the supernatant, add 100 µL ice-cold PBS to resuspend and culture at 100 ℃ for 5 min and 186 µL cold anhydrous ethanol was added to the boiling material, whirl for 15 s, then centrifuge at 4 ℃ and 16000 g for 2 min, take the supernatant to a new microcentrifuge tube and store it temporarily at -20 ℃. The precipitate was processed twice, and the supernatant obtained three times was combined and dried in a vacuum concentrator in 45 ℃ for 4 h. The white particles contained c-di-GMP, were stored at -80 ℃. The total protein of the precipitate concentration was measured after ultrasonic fragmentation, and the protein concentration was used for normalization (Petrova and Sauer 2017).

2.8.2 c-di-GMP detection by HPLC

The precipitate containing c-di-GMP (Sigma-Aldrich, St Louis, USA) is dissolved in 1 mL of ultra-pure water and filtered through the 0.45 μm hydrophobic PTFE filter, and the c-di-GMP standard substance is configured with a concentration gradient of 2.5, 5, 10, 20, 40 pmol/mL, which also needs to be filtered. Samples were detected by high performance liquid chromatography (Waters, MA, USA), specific parameters including Reverse-phase C_{18} column (4.6×250 mm, 5 μm, Elite Ltd, Dalian, China), HPLC solvent (90%: 10 mM ammonium acetate solution, and 10%: 10 mM ammonium acetate methanol solution), column temperature (60 ℃), flow velocity (1 mL/min). Normalize c-di-GMP levels to total cellular protein levels (i.e. pmol/mg) by using the fitted standard curve.

2.9 RNA extraction and real-time quantitative polymerase chain reaction (RT-qPCR)

Bacterial strains were cultured at 30 ℃ and 37 ℃, respectively, until the OD_{600} = 2.0, i.e. 2×10^9 CFUs of bacteria. Total RNA was extracted by the TRIzol method as described before (Duan et al. 2013). Concentration and purity of RNA was detected through NanoDrop ND-1000 spectrophotometer (Thermo Fisher Scientific, MA, USA) and agarose gel electrophoresis, respectively. And the cDNA was synthesized via the PrimeScriptRT reagent Kit (Takara, Shiga, Japan) for reverse transcription-PCR. The amplification sequence of primers for RT-qPCR is shown in Table 2. Then the qRT-PCR test is performed according to the SYBRPremix Ex Taq™ Perfect Real Time (Takara, Shiga, Japan) on an Applied Biosystems 7500 Real Time System. The data obtained by qRT-PCR were analyzed by $2^{-\Delta\Delta CT}$ method(Livak and Schmittgen 2000), and then transformed into $\log_2$ to show fold-change differences among each bacterial strains.

Table 2
The sequence of primers for RT-qPCR

gene	forward primer	reverse primer
gapA	GTTGTCGCTGAAGCAACTGG	ACCGGTAGAAGACGGGATGA
nirC	TGGTATCGCCTTAACGCTGG	TGTACGCAATGCCATCCAGA
rpoS	GCTCGAACAGCCATTTGACG	ACGTGGTTTCCGCTTCTCAA
csrA	GACCCTCATGATTGGGGATGA	GCCTGGATACGCTGGTAGATC
narP	TCCAGCGATGTCTTTGCACT	CGGACGTTGAGTTTACGCAG
pgaC	GTGCCGTAACCGGTAATCCT	GAATACTTCTGCACCGCCCT
bcsA	AGTGTGCGCATCTTCGGTTA	TATGCCAAAGGCGAGTTCGT
csgA	ACATTTACCAGTACGGTGGCG	ATGAGCGGTCGCGTTGTTA
fimA	ACCCACGACGGTAAATGGTG	CTGCACTAAATGTCGCACCG
dcgT	GGGCCGATAGTTGCTCACAT	CGCGATGTGCAATGTCCTTT

2.10 Statistical analysis

GraphPad Prism (San Diego, CA, USA) version 8 (a simple t-test analysis or one-way analysis for multiple comparisons) were used for estimating statistical significance. And it's defined as $P < 0.05$ (represented by *), $P < 0.01$ (represented by **), $P < 0.001$(represented by ***), and $P < 0.0001$ (represented by ****).

3 Results

3.1 Genetic stability and growth characteristics

According to the PCR and DNA sequence results, we confirmed the construction of Δ*nirC* and Δ*nirC*/p*nirC*, and there are no point mutations in the complemented strain. PCR identification results showed in supporting material 1. The growth curves of these three strains showed no obvious differences at 30 ℃ or 37 ℃, indicating that the deletion of *nirC* gene had no effect on the growth of bacteria (Fig. 1).

3.2 Knockout of *nirC* gene changes the motility, biofilm formation, and adhesion ability of APEC XM

The Δ*nirC* showed a larger motion ring than WT at 30 ℃ and 37 ℃, especially at 37 ℃ (Fig. 2). We detected the biofilm formation of each strain at 30 ℃ and 37 ℃, and found that the biofilm formation level of Δ*nirC* decreased about 55.7% at 30 ℃ compared with WT, but this function was restored at 37 ℃ (Fig. 3). In order to maintain cell viability, we only detected the adhesion level of bacterial strains to bEnd.3 cells at 37 ℃. The results showed that the adhesion ability of Δ*nirC* was significantly lower than that of wild strains, about 30.3% (Fig. 4).

3.3 Colony morphology of Δ*nirC* on Congo red plate is different with wild type

Colony morphology of Δ*nirC* grown on Congo red plate exhibited a white and smooth form at 30 ℃ and 37 ℃, especially at 30 ℃ (Fig. 5), while the WT and Δ*nirC*/p*nirC* showed red, dry and routh (rdar) phenotype. The results show that the genes expression of cellulose and Curli is significantly down-regulated in Δ*nirC*.

3.4 Deletion of *nirC* gene leads to the decrease of intracellular c-di-GMP concentration of APEC XM

The results of HPLC detection of c-di-GMP were consistent with colony morphology test for each bacterial strains. The intracellular c-di-GMP concentration of Δ*nirC* was about 25.1% lower than that of WT at 30 ℃, and this result decreased by 15.1% at 37 ℃ (Fig. 6).

3.5 Expression level of regulatory and phenotypic genes in NirC-deficient mutant

RT-qPCR was used to detect the transcription level of regulatory factors, including RNA polymerase sigma S subunit gene *rpoS*, carbon storage regulator gene *csrA*, two-component systems response regulator gene *narP*, and diguanylate cyclase gene *dgcT*. The phenotypic genes include Curli A subunit gene *csgA*, cellulose synthase A subunit gene *bcsA*, N-acetylglucosamine synthase large subunit gene *pgaC*, and type I fimbriae main subunit gene *fimA*.

At 30 ℃, the expression level of *rpoS* and *csrA* of Δ*nirC* was up-regulated about 258% and 213% when compared with WT, respectively, *narP* and *dgcT* was down-regulated by both 37% (Fig. 7A). Meanwhile, the expression of *csgA*, *bcsA*, *pgaC* and *fimA* genes were down-regulated by 30%, 47 %, 29% and 51 % when compared with WT (Fig. 7B). At 37 ℃, the results changed, both *rpoS* and *narP* of Δ*nirC* maintained the significant difference, compared with WT, *rpoS* was up-regulated by 140 % while *narP* was down-regulated by 27%. There was no statistical difference in the expression level of *csrA*, *dgcT*, *csgA*, *bcsA*, *pgaC* and *fimA* genes, but the trend of *csrA* and *dgcT* expression was similar with the result at 30 ℃ (Fig. 7C and 7D).

4 Discussion

As a NO_2^- transport channel, NirC absence means high concentrations of NO_2^- can not be transported into the cell and accumulated outside. It is a dangerous signal for bacteria since the conjugate acid of NO_2^-, free nitrous acid, can make free diffusion across the cytomembrane and produce reactive nitrogen species such as NO and caused oxidative damage(Hartop et al. 2017). Our result shows the counter-measures of *E. coli* in response to this emergency, comparing with WT, Δ*nirC* demonstrated a strong swimming with lower biofilm (or biofilm component) production and adhesion ability, which suggested that the bacteria seem to escape the adverse environment.

RpoS is a sigma subunit of RNA polymerase complex and a global stress regulator involved in abiotic stress responses, such as oxidative stress, nutrient limitation, and so on (Sedlyarova et al. 2016). In theory, the deletion of *nirC* gene results in a large number of NO_2^- accumulate outside is a kind of stress to the bacteria, called nitrite stress. This explains why the *nirC* mutant leads to a significant increase in *rpoS* expression in this study. NarP is the effector of the two-component regulatory system in response to nitrite/nitrate stimulation, and regulates the expression of periplasmic and cytoplasmic nitrite reductase system (Noriega et al. 2010). RpoS negatively regulates the expression of *narP* through sRNA SdsN137 and SdsN178 (Hao et al. 2016). In the present study, we found the expression levels of *narP* was down-regulated significantly while *rpoS* gene was up-regulated, and these findings were consistent with previous findings. CsrA is a homologous dimer RNA binding protein, which participates in carbon metabolism, motility, and biofilm formation of *E. coli*(Jonas et al. 2008). Studies have shown that CsrA is regulated and activated by RpoS (Park et al. 2017; Yakhnin et al. 2011), and CsrA negatively regulates the content of c-di-GMP by specifically binding to the promoter of diguanosine cyclase gene *dgcT* (formerly known as *ycdT*) (Hengge et al. 2016). Through RT-qPCR and HPLC methods, we proved that after the deletion of *nirC* gene, the expression of *rpoS* and *csrA* was up-regulated, and the content of c-di-GMP in

bacteria was decreased, which supported the above theory. Thus, we found a pathway to regulate *E. coli* nitrite stress.

E. coli mainly relied on flagella in their motility. Flagellar molecular brake protein YcgR has a PilZ domain, can be activated by c-di-GMP to inhibit flagellar rotor proteins MotA, thus curbing flagellar motor output (Boehm et al. 2010). Biofilm is a group of microorganisms surrounded by extracellular polymer matrix at the interface(Flemming and Wingender 2010). Extracellular polymers are usually composed of extracellular polysaccharides, secretory proteins, and DNA, in which the synthesis of cellulose, poly N-acetylglucosamine, and Curli is regulated by c-di-GMP(Steiner et al. 2013; Wang et al. 2004). Our results showed that the increased motility and the decrease of biofilm formation ability of *nirC* mutant were consistent with the decrease of c-di-GMP content in bacteria. Type I fimbria is a very important adhesin in *E. coli* (Mulvey et al. 1998). Although there have not been reported that type I fimbria is regulated by c-di-GMP in *E. coli*, our results show that the expression of *fimA* is down-regulated when the content of c-di-GMP decreases. Whether c-di-GMP is involved in the regulation of type I fimbriae needs to be further explored. In view of type I fimbriae is an important virulence factor of meningitis-caused *E. coli*, deletion of *nirC* gene decreased the adhesion ability, suggesting that nitrite stress can significantly reduce the pathogenicity of APEC XM.

5 Conclusion

We proposed that nitrite stress is the directed reason for the change of biological characteristics of APEC XM caused by *nirC* gene deletion, and we put forward a possible signal regulatory pathway. The deletion of *nirC* gene leads to nitrite stress, and then the expression level of stress regulator *rpoS* is up-regulated and further activates the transcription of *csrA*. CsrA inhibits the expression of *dgcT* and thus reduces the concentration of c-di-GMP in bacteria. At low levels of c-di-GMP, APEC XM show enhanced motility, reduced biofilm formation, and reduced adhesion ability. In addition, our results show that nitrite stress becomes stronger at a low temperature, a model of this mechanism is shown in Fig. 8.

Abbreviations

***E. coli*:** *Escherichia coli*

APEC: avian pathogenic *Escherichia coli*

c-di-GMP: 3',5'-cyclic diguanosine monophosphate

NMEC: neonatal meningitis *Escherichia coli*

NO_2^-: nitrite

NO: nitric oxide

$ONOO^-$: peroxynitrite anion

HPLC: high performance liquid chromatography

LB: Luria-Bertani

DMEM: Dulbecco's modified Eagle's medium

FBS: fetal bovine serum

OD_{600}: optical density at 600 nm

MOI: multiplicity of infection

CFU: colony-forming unit

DMSO: dimethyl sulfoxide

rdar: red, dry, and rough

MTT: methyl thiazolyl tetrazolium

PCR: polymerase chain reaction

RT-qPCR: Real-time quantitative PCR

Declarations

Acknowledgement: The authors gratefully acknowledge Professor Lu Chengping, Nanjing Agricultural University, College of Veterinary Medicine for providing the APEC XM strain for this study.

Funding: This work was supported by Graduates Research & Practice Innovation Program of Yangzhou University No. KYCX20_3004, College Students Research & Practice Innovation Program, International Collaboration Program from Science and Technology Agency of Jiangsu Province (2019), the Priority Academic Program Development of Jiangsu Higher Education Institutions.

Conflicts of interest/Competing interests: Not applicable

Ethics approval: Not applicable

Consent to participate: Not applicable

Consent for publication: Not applicable

Availability of data and material: Not applicable

Code availability: Not applicable

Authors' contributions: JL and DZ performed the experiments, analyzed the data, and wrote the manuscript. SL, XG, and QH participated in the data analysis and wrote the paper. PX and GZ conceived and designed the study, participated in experimental work, and wrote the paper. All authors read and approved the final manuscript.

References

1. Boehm A, Kaiser M, Li H, Spangler C, Kasper CA, Ackermann M, Kaever V, Sourjik V, Roth V, Jenal U (2010) Second Messenger-Mediated Adjustment of Bacterial Swimming Velocity. Cell 141(1):107-116 doi:10.1016/j.cell.2010.01.018
2. Carlsson S, Wiklund NP, Engstrand L, Weitzberg E, Lundberg JON (2001) Effects of pH, nitrite, and ascorbic acid on nonenzymatic nitric oxide generation and bacterial growth in urine. Nitric Oxide-Biol Ch 5(6):580-586 doi:10.1006/niox.2001.0371
3. Cheang QW, Xin L, Chea RYF, Liang Z-X (2019) Emerging paradigms for PilZ domain-mediated C-di-GMP signaling. Biochem Soc T 47:381-388 doi:10.1042/bst20180543
4. Clegg S, Yu F, Griffiths L, Cole JA (2002) The roles of the polytopic membrane proteins NarK, NarU and NirC in Escherichia coli K-12: two nitrate and three nitrite transporters. Mol Microbiol 44(1):143-155 doi:10.1046/j.1365-2958.2002.02858.x
5. Das P, Lahiri A, Lahiri A, Chakravortty D (2009) Novel role of the nitrite transporter NirC in Salmonella pathogenesis: SPI2-dependent suppression of inducible nitric oxide synthase in activated macrophages. Microbiol-Sgm 155:2476-2489 doi:10.1099/mic.0.029611-0
6. Datsenko KA, Wanner BL (2000) One-step inactivation of chromosomal genes in Escherichia coli K-12 using PCR products. P Natl Acad Sci USA 97(12):6640-6645 doi:10.1073/pnas.120163297
7. de Paiva JB, Leite JL, Mendes da Silva LP, Galvao Rojas TC, de Pace F, Conceicao RA, Sperandio V, da Silveira WD (2015) Influence of the major nitrite transporter NirC on the virulence of a Swollen Head Syndrome Avian Pathogenic E. coli (APEC) strain. Vet Microbiol 175(1):123-131 doi:10.1016/j.vetmic.2014.11.015
8. Dho-Moulin M, Fairbrother JM (1999) Avian pathogenic Escherichia coli (APEC). Vet Res 30(2-3):299-316
9. Duan Q, Zhou M, Zhu X, Yang Y, Zhu J, Bao W, Wu S, Ruan X, Zhang W, Zhu G (2013) Flagella from F18+Escherichia coli play a role in adhesion to pig epithelial cell lines. Microb Pathogenesis 55:32-38 doi:10.1016/j.micpath.2012.09.010
10. Flemming HC, Wingender J (2010) The biofilm matrix. Nat Rev Microbiol 8(9):623-33 doi:10.1038/nrmicro2415
11. Hao Y, Updegrove TB, Livingston NN, Storz G (2016) Protection against deleterious nitrogen compounds: role of sigma(S)-dependent small RNAs encoded adjacent to sdiA. Nucleic Acids Res 44(14):6935-6948 doi:10.1093/nar/gkw404

12. Hartop KR, Sullivan MJ, Giannopoulos G, Gates AJ, Bond PL, Yuan Z, Clarke TA, Rowley G, Richardson DJ (2017) The metabolic impact of extracellular nitrite on aerobic metabolism of Paracoccus denitrificans. Water Res 113:207-214 doi:10.1016/j.watres.2017.02.011
13. Hejair HMA, Zhu Y, Ma J, Zhang Y, Pan Z, Zhang W, Yao H (2017) Functional role of ompF and ompC porins in pathogenesis of avian pathogenic Escherichia coli. Microb Pathogenesis 107:29-37 doi:10.1016/j.micpath.2017.02.033
14. Hengge R (2009) Principles of c-di-GMP signalling in bacteria. Nat Rev Microbiol 7(4):263-73 doi:10.1038/nrmicro2109
15. Hengge R, Galperin MY, Ghigo J-M, Gomelsky M, Green J, Hughes KT, Jenal U, Landini P (2016) Systematic Nomenclature for GGDEF and EAL Domain-Containing Cyclic Di-GMP Turnover Proteins of Escherichia coli. J Bacteriol 198(1):7-11 doi:10.1128/jb.00424-15
16. Hossain MM, Tsuyumu S (2006) Flagella-mediated motility is required for biofilm formation byErwinia carotovorasubsp.carotovora. J Gen Plant Pathol 72(1):34-39
17. Jain S, Chen JR (2006) Antibiotic resistance profiles and cell surface components of salmonellae. J Food Protect 69(5):1017-1023 doi:10.4315/0362-028x-69.5.1017
18. Jia W, Tovell N, Clegg S, Trimmer M, Cole J (2009) A single channel for nitrate uptake, nitrite export and nitrite uptake by Escherichia coli NarU and a vole for NirC in nitrite export and uptake. Biochem J 417:297-304 doi:10.1042/bj20080746
19. Jonas K, Edwards AN, Simm R, Romeo T, Romling U, Melefors O (2008) The RNA binding protein CsrA controls cyclic di-GMP metabolism by directly regulating the expression of GGDEF proteins. Mol Microbiol 70(1):236-57 doi:10.1111/j.1365-2958.2008.06411.x
20. Khlebodarova TM, Ree NA, Likhoshvai VA (2016) On the control mechanisms of the nitrite level in Escherichia coli cells: the mathematical model. BMC Microbiol 16 doi:10.1186/s12866-015-0619-x
21. Livak K, Schmittgen T (2000) Analysis of Relative Gene Expression Data Using Real-Time Quantitative PCR and the 2-△△Ct Method. Methods 25(4)
22. Lu W, Schwarzer NJ, Du J, Gerbig-Smentek E, Andrade SLA, Einsle O (2012) Structural and functional characterization of the nitrite channel NirC from Salmonella typhimurium. P Natl Acad Sci USA 109(45):18395-18400 doi:10.1073/pnas.1210793109
23. Ma J, Bao Y, Sun M, Dong W, Pan Z, Zhang W, Lu C, Yao H (2014) Two Functional Type VI Secretion Systems in Avian Pathogenic Escherichia coli Are Involved in Different Pathogenic Pathways. Infect Immun 82(9):3867-3879 doi:10.1128/iai.01769-14
24. Mulvey MA, Lopez-Boado YS, Wilson CL, Roth R, Parks WC, Heuser J, Hultgren SJ (1998) Induction and evasion of host defenses by type 1-piliated uropathogenic Escherichia coli. Science (Washington D C) 282(5393):1494-1497 doi:10.1126/science.282.5393.1494
25. Noriega CE, Lin H-Y, Chen L-L, Williams SB, Stewart V (2010) Asymmetric cross-regulation between the nitrate-responsive NarX-NarL and NarQ-NarP two-component regulatory systems from Escherichia coli K-12. Mol Microbiol 75(2):394-412 doi:10.1111/j.1365-2958.2009.06987.x

26. Park H, McGibbon LC, Potts AH, Yakhnin H, Romeo T, Babitzke P (2017) Translational Repression of the RpoS Antiadapter IraD by CsrA Is Mediated via Translational Coupling to a Short Upstream Open Reading Frame. Mbio 8(4) doi:10.1128/mBio.01355-17
27. Pesavento C, Becker G, Sommerfeldt N, Possling A, Tschowri N, Mehlis A, Hengge R (2008) Inverse regulatory coordination of motility and curli-mediated adhesion in Escherichia coli. Gene Dev 22(17):2434-2446 doi:10.1101/gad.475808
28. Petrova OE, Sauer K (2017) High-Performance Liquid Chromatography (HPLC)-Based Detection and Quantitation of Cellular c-di-GMP. Methods in molecular biology (Clifton, NJ) 1657:33-43 doi:10.1007/978-1-4939-7240-1_4
29. Rycovska A, Hatahet L, Fendler K, Michel H (2012) The nitrite transport protein NirC from Salmonella typhimurium is a nitrite/proton antiporter. BBA-Biomembranes 1818(5):1342-1350 doi:10.1016/j.bbamem.2012.02.004
30. Sedlyarova N, Shamovsky I, Bharati BK, Epshtein V, Chen J, Gottesman S, Schroeder R, Nudler E (2016) sRNA-Mediated Control of Transcription Termination in E-coli. Cell 167(1):111-+ doi:10.1016/j.cell.2016.09.004
31. Simm R, Morr M, Kader A, Nimtz M, Romling U (2004) GGDEF and EAL domains inversely regulate cyclic di-GMP levels and transition from sessility to motility. Mol Microbiol 53(4):1123-1134 doi:10.1111/j.1365-2958.2004.04206.x
32. Steiner S, Lori C, Boehm A, Jenal U (2013) Allosteric activation of exopolysaccharide synthesis through cyclic di-GMP-stimulated protein-protein interaction. EMBO J 32(3):354-68 doi:10.1038/emboj.2012.315
33. Wang HN, Gunsalus RP (2000) The nrfA and nirB nitrite reductase operons in Escherichia coli are expressed differently in response to nitrate than to nitrite. J Bacteriol 182(20):5813-5822 doi:10.1128/jb.182.20.5813-5822.2000
34. Wang X, Preston JF, Romeo T (2004) The pgaABCD Locus of Escherichia coli Promotes the Synthesis of a Polysaccharide Adhesin Required for Biofilm Formation. J Bacteriol 186(9):2724-2734 doi:10.1128/jb.186.9.2724-2734.2004
35. Yakhnin H, Yakhnin AV, Baker CS, Sineva E, Berezin I, Romeo T, Babitzke P (2011) Complex regulation of the global regulatory gene csrA: CsrA-mediated translational repression, transcription from five promoters by E sigma(70) and E sigma(S), and indirect transcriptional activation by CsrA. Mol Microbiol 81(3):689-704 doi:10.1111/j.1365-2958.2011.07723.x

Figures

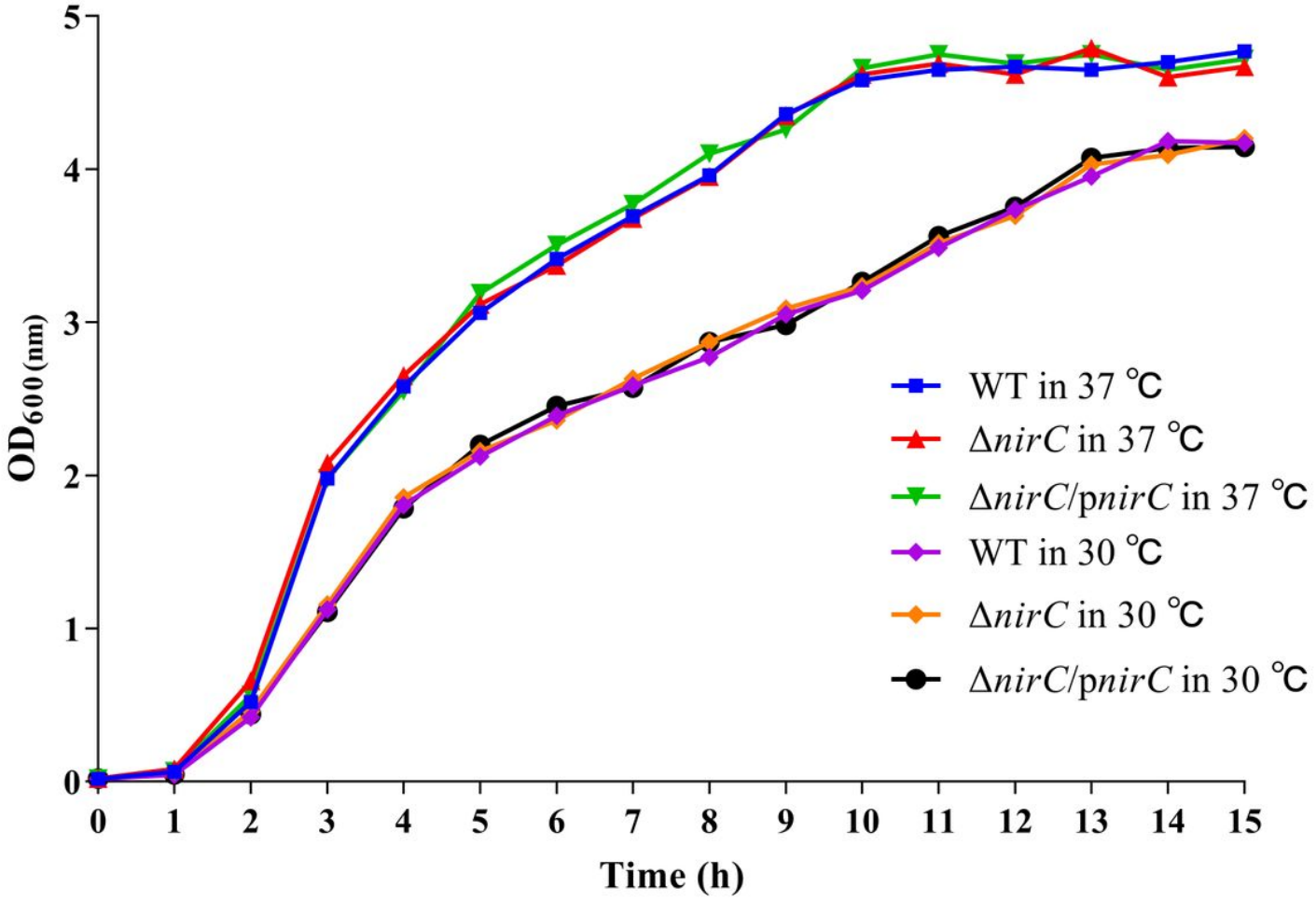

Figure 1

Bacterial growth characteristics at 30 ℃ and 37 ℃. The growth characteristics of WT, ΔnirC and ΔnirC/pnirC were consistent at 30 ℃ or 37 ℃. We chose 30 ℃ for experiments because the enzymatic activity of extracellular nitrite reductase was low, extracellular nitrite accumulated more easily which can cause stronger stimulation. 37 ℃ is the body temperature of the model host (mouse) of the strains.

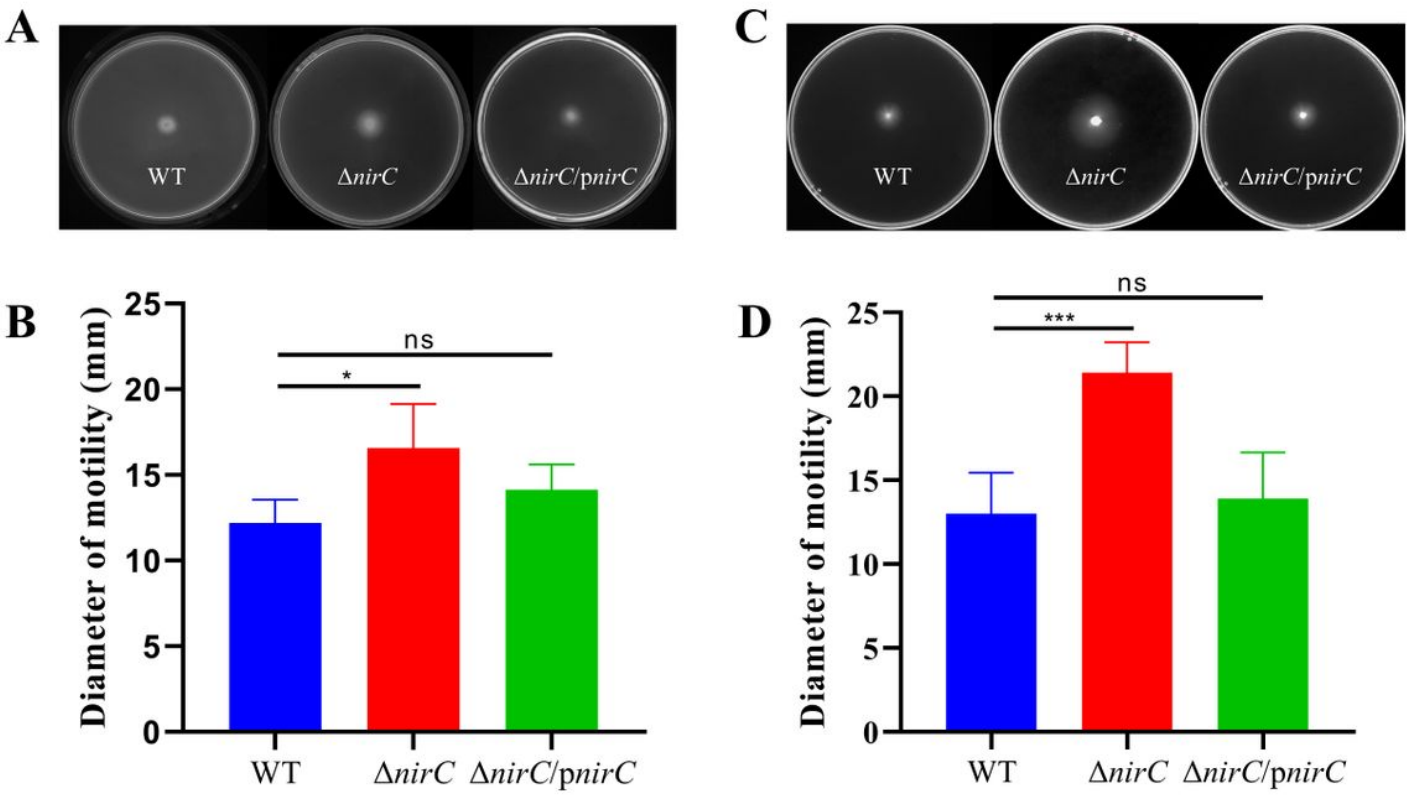

Figure 2

Bacterial motility test at 30 °C (A and B) and 37 °C (C and D). The swimming ring diameter of ΔnirC was larger than that of the WT, whether at 30 °C or 37 °C. ns: not significant.

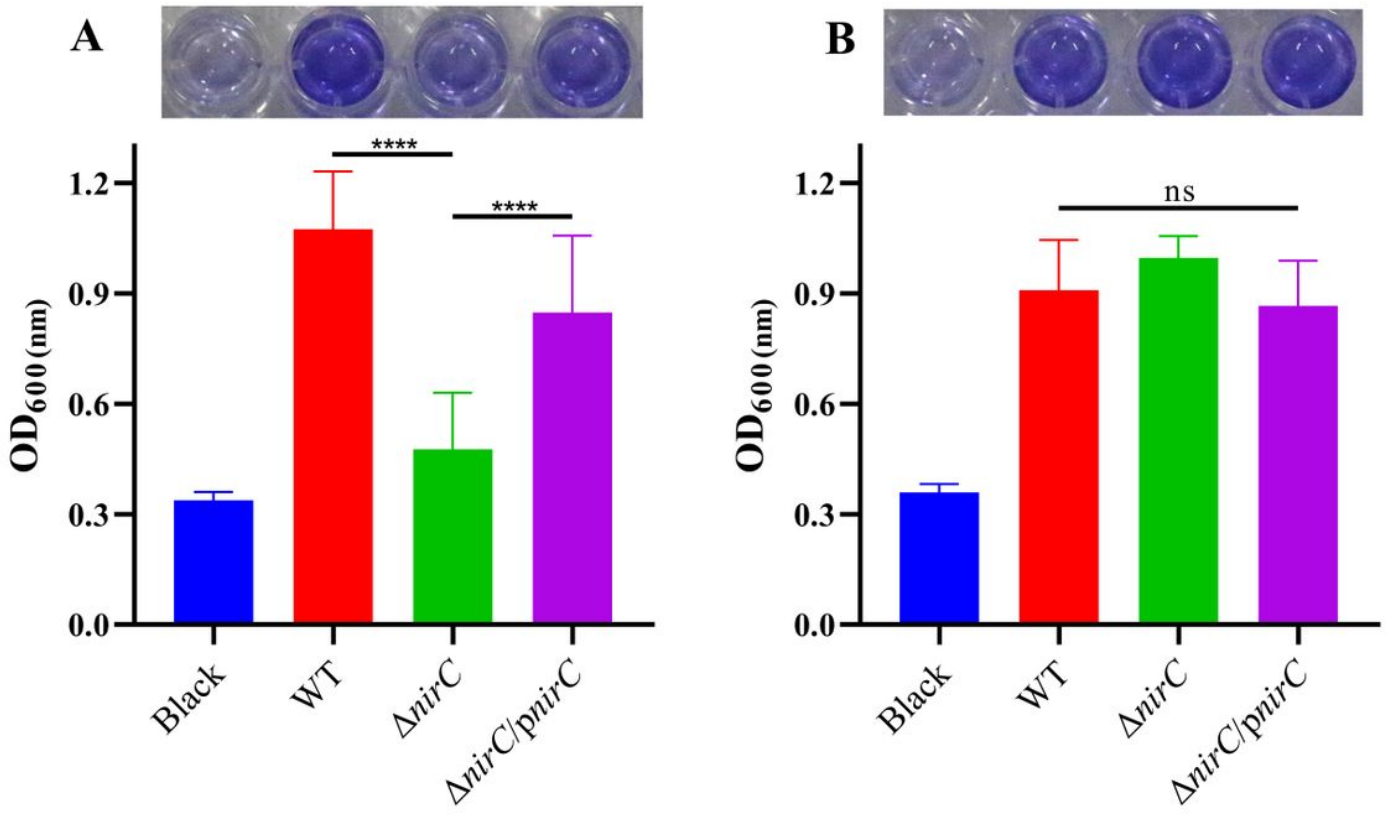

Figure 3

Bacterial biofilm formation test at 30 ℃ (A) and 37 ℃ (B). The biofilm formation ability of ΔnirC was decreased at 30 ℃, but there was no significant difference of biofilm formation at 37 ℃.

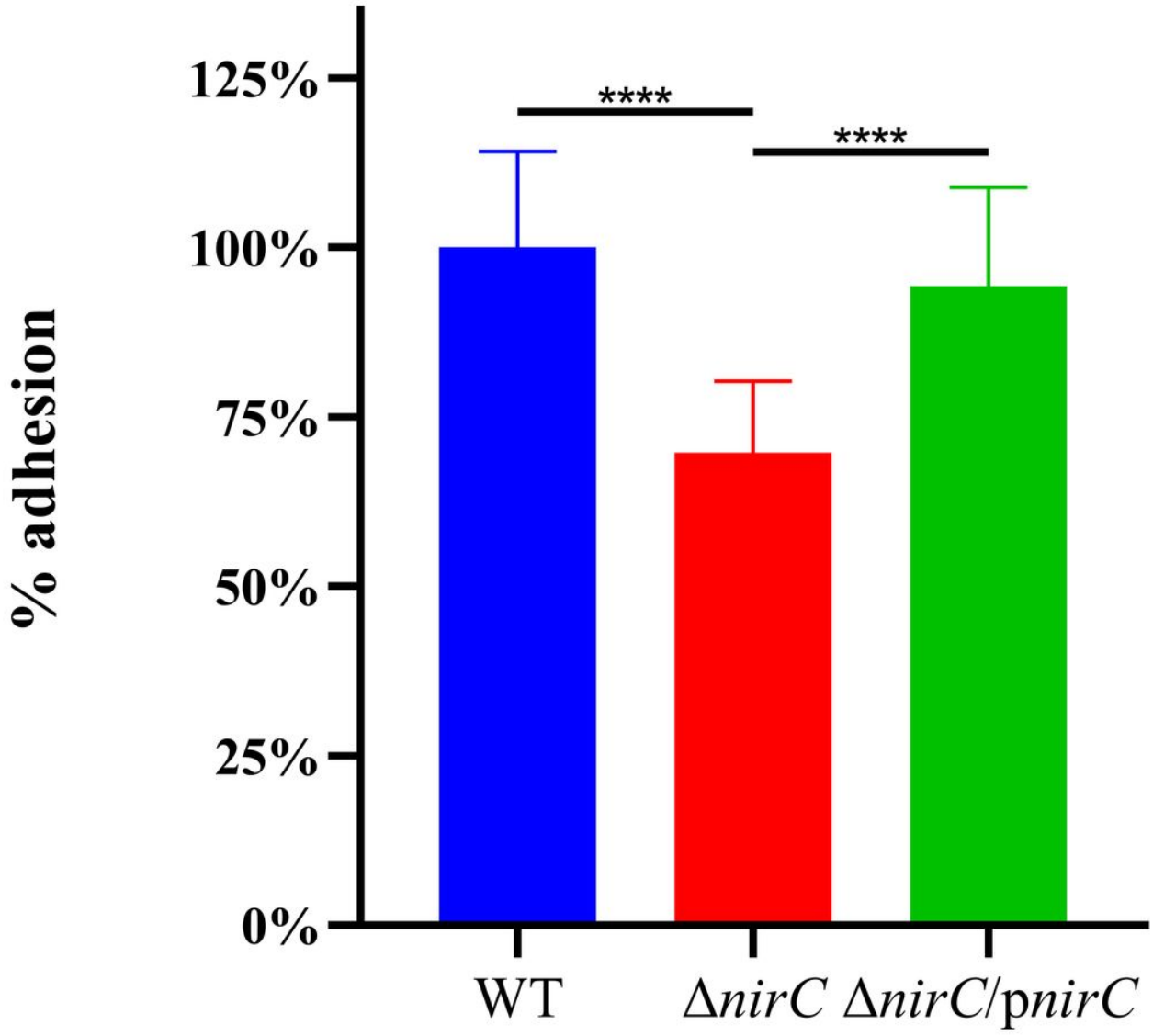

Figure 4

Bacterial adhesion test on b.End3 cell. The adhesion ability of ΔnirC to the b.End3 cells decreased, and we only tested it at 37 ℃, since the cell activity was seriously affected at 30 ℃.

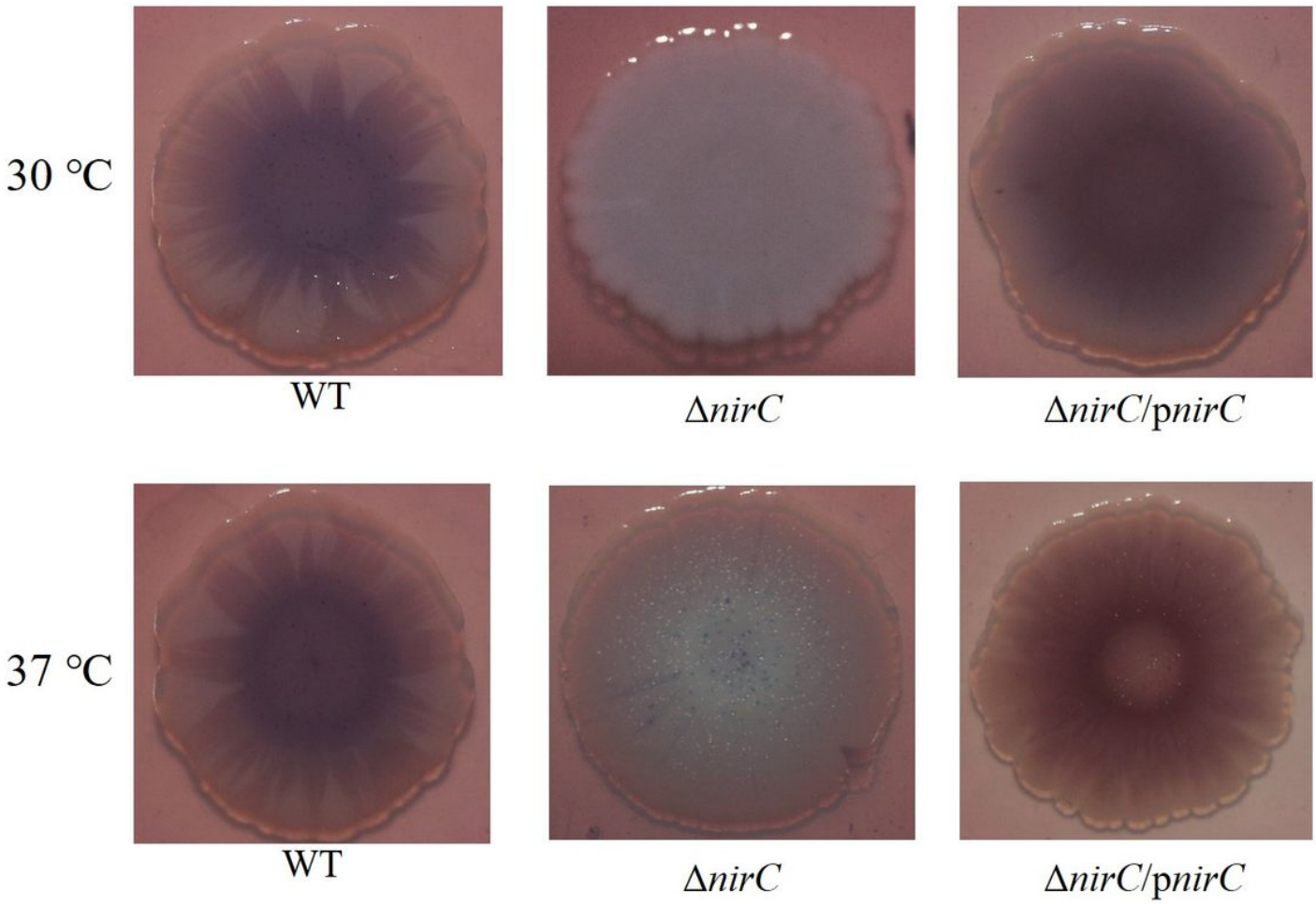

Figure 5

Bacterial colony morphology on Congo red-Coomassie brilliant blue plate. ΔnirC showed a white and smooth phenotype at 30 °C and 37 °C while WT and ΔnirC/pnirC was red dry and rough phenotypes.

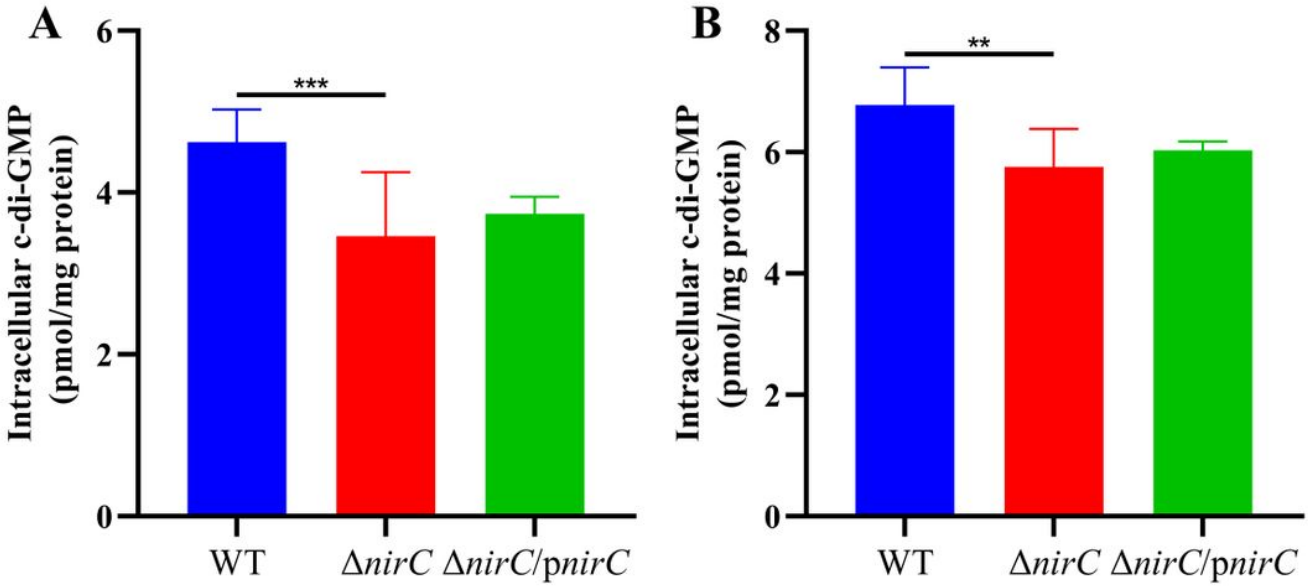

Figure 6

Bacterial intracellular c-di-GMP detection at 30 °C (A) and 37 °C (B).

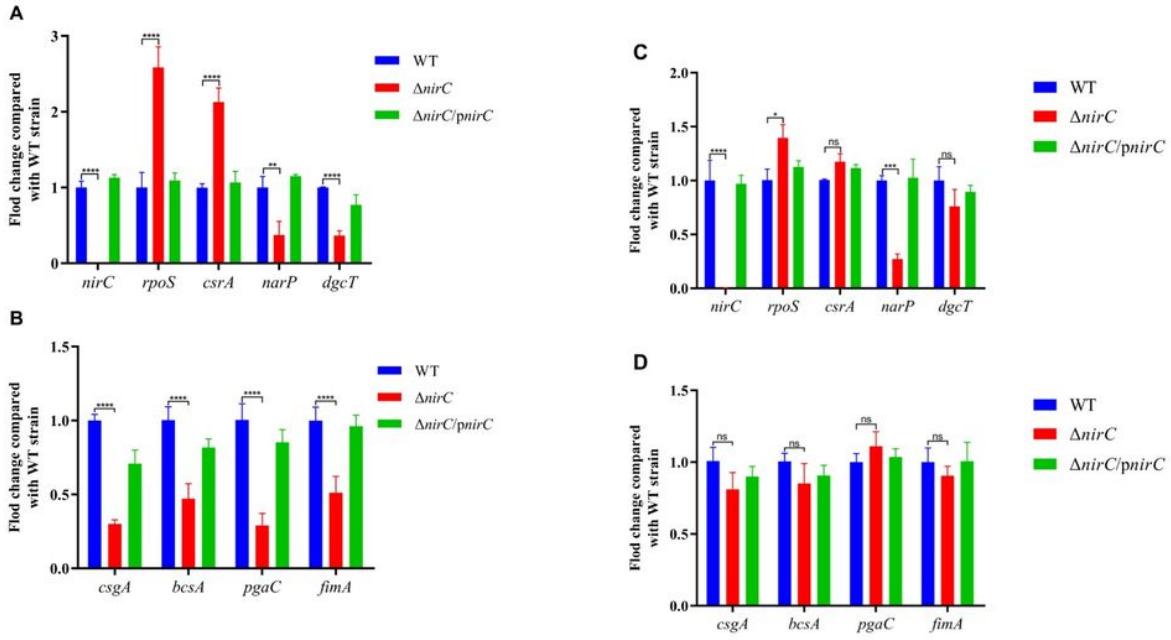

Figure 7

Gene expression detection at 30 ℃ (A and B) and 37 ℃ (C and D). Regulatory genes: rpoS, csrA, narP and dgcT. Phenotypic genes: csgA, bcsA, pgaC and fimA.

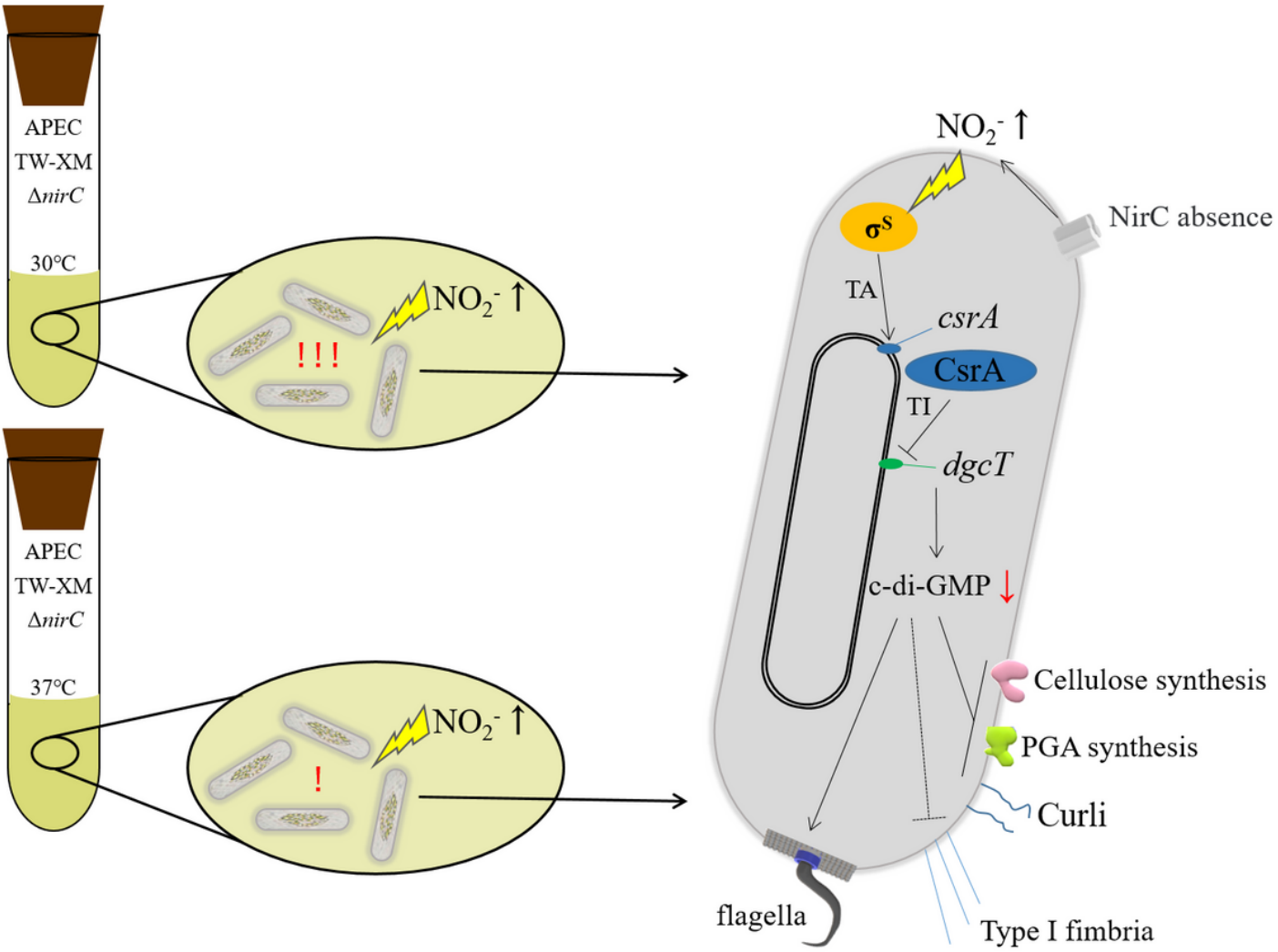

Figure 8

A model of nitrite stress caused by nirC deletion. After nirC gene was deleted, NO2- is accumulated and leads to nitrite stress, and then the expression of stress regulator rpoS is up-regulated and further activates the transcription of csrA. CsrA inhibits the expression of dgcT and thus reduces the content of c-di-GMP in bacteria. Due to flagella, cellulose, Curli, and PGA are regulated by c-di-GMP, so bacteria show enhanced motility and a low level of biofilm formation ability. Moreover, our results show that nitrite stress becomes stronger at a low temperature. σS: RNA polymerase sigma subunit S (RpoS); TA: transcriptional activation; TI: transcription inhibition; PGA: poly N-acetylglucosamine

Supplementary Files

This is a list of supplementary files associated with this preprint. Click to download.

- S1PCRidentification.tif